Neurospectral Computation for the Resonant Characteristics of an Equilateral Triangular Patch Antenna on Suspended Substrates

Ahmed Mahamdi
LHS Laboratory, Electronics Department, University of Freres Mentouri - Constantine 1, Constantine, Algeria | Institute of Science and Applied Technology, University of Larbi Ben M'hidi, Oum El Bouaghi, Algeria
mahamdi.ahmed@univ-oeb.dz (corresponding author)

Skander Aris
LHS Laboratory, Electronics Department, University of Frères Mentouri - Constantine 1, Constantine, Algeria
aris.skander@umc.edu.dz

Tarek Fortaki
LEA Laboratory, Electronics Department, University of Batna 2, Batna, Algeria
t.fortaki@univ-batna2.dz

Siham Benkouda
LHS Laboratory, Electronics Department, University of Freres Mentouri - Constantine 1, Constantine, Algeria
siham.benkouda@umc.edu.dz

Sami Bedra
Industrial Engineering Department, University of Khenchela, Khenchela, Algeria
bedra_sami@univ-khenchela.dz

Received: 8 September 2024 | Revised: 13 October 2024 | Accepted: 26 October 2024

 DOI: https://doi.org/10.48084/etasr.8930

ABSTRACT

Modeling and design of an equilateral triangular patch antenna on suspended and single substrate are accomplished in this paper. The spectral domain approach is important due to its accuracy, but has a high computational cost. On the other hand, the Artificial Neural Networks (ANNs) have recently become a fast and flexible vehicle for modeling and designing microwave antennas. This paper introduces electromagnetic knowledge combined with ANNs to compute the resonant frequency of the fundamental and higher order modes and to eliminate the difficulties of handling the singularity points encountered in the numerical evaluation of integrals. The resonant frequency results obtained from the neural model are in very good agreement with the experimental and theoretical results available in the literature.

Keywords-triangular microstrip antenna; artificial neural networks; modeling and design; spectral domain analysis

I. INTRODUCTION

Triangular microstrip patch antennas printed on isotropic substrates have been extensively analyzed [1, 2]. Using the cavity model, the geometry is versatile to be compatible over a curved surface and also physically smaller compared to other common patch shapes. Several micro strip patch investigations reported in open literature include basic modal analysis and computer aided design [3]. The introduction of tenability through miniaturization and metamaterial utilization, the achievement of dual band or circular polarized features through the use of slots and shorting pins, and the creation of multilayered stacked geometry have been discussed [4]. Although, the moment method provides better accuracy [5, 6],

as a full-wave method, it is computational-intensive. Due to the presence of poles in the integral path, it is difficult to integrate the Green function numerically. The increase in the complexity of device modeling has led to rapid growth in the field of computational modeling research.

Because of these problems, researchers use artificial intelligence techniques to find better solutions [7]. Authors in [8] introduced the use of neural networks in conjunction with the Spectral Domain approach (SDA). Fast neural models trained from measured and simulated microwave data can be used during microwave design to provide immediate answers to the task they learned [9, 10]. The neural modeling of nonlinear characteristics of the device circuit has become an important research area used to solve nonlinear computing problems [11, 12].

This paper exhibits the use of neural network technology for the purpose of analysis. The ANN technique determines the resonant frequency of an equilateral triangular patch antenna in combination with the spectral domain formulation and the effect of suspended and single substrate on the resonant frequency of an equilateral triangular patch antenna. The current model is in very close agreement with the experimental and numerical results. Finally, the commercial software CST was utilized to validate the present neurospectral approach. To the best of our knowledge, this subject has not been reported in the open literature.

II. THEORETICAL BACKGROUND

The geometry under consideration, i.e. a triangular patch on a suspended and single substrate, is illustrated in Figure 1. The suspended substrate consists of two dielectric substrates. The first one is an air gap with constitutive parameters ε_0 and μ_0, while the second one is a dielectric material with permittivity εr and permeability μ_0. To simplify the analysis, the antenna feed will not be considered. All fields and currents are time-harmonic with the e^{iwt} time dependence suppressed. The cross-fields within the j^{th} layer (j = 1, 2) can be obtained via the Fourier transform reverse vector as [7]:

$$E(r_s,z)= \begin{bmatrix} Ex(rs,z) \\ Ey(rs,z) \end{bmatrix} = \frac{1}{4\pi^2}\int_{-\infty}^{+\infty}\int_{-\infty}^{+\infty} \bar{F}\,(k_s,r_s)h(k_s,z)dk_x dk_y \quad (1)$$

$$H(rs,z) = \begin{bmatrix} Hy(rs,z) \\ -Hx(rs,z) \end{bmatrix} = \frac{1}{4\pi^2}\int_{-\infty}^{+\infty}\int_{-\infty}^{+\infty} \bar{F}\,(k_s,r_s)e(k_s,z)dk_x dk_y \quad (2)$$

where $\bar{F}\,(k_s,r_s)$ is the kernel of the Fourier transform [7] vector, and we obtain the matrix form [9]:

$$\begin{bmatrix} e(k_s,d^-) \\ h(k_s,d^-) \end{bmatrix} = \bar{T}\cdot\begin{bmatrix} e(k_s,0^+) \\ h(k_s,0^+) \end{bmatrix} \quad (3)$$

with:

$$\bar{T} = \begin{bmatrix} \bar{T}^{11} & \bar{T}^{12} \\ \bar{T}^{21} & \bar{T}^{22} \end{bmatrix} = \begin{bmatrix} \bar{I}\cos\bar{\theta} & -i\,g^{-1}\sin\bar{\theta} \\ -i\,\bar{g}\sin\bar{\theta} & \bar{I}\cos\bar{\theta} \end{bmatrix} \quad (4)$$

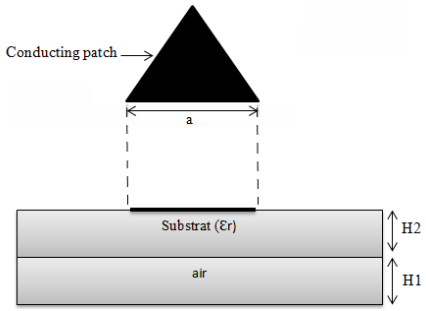

Fig. 1. The triangular MSA structure.

Equation (4) combines e and h on both sides of the j^{th} layer as input and output quantities. It is then easy to derive the dyadic Green's function of the problem in a manner very similar to that shown in [13-15]. G(ks) is the dyadic Green's function in the Fourier transform vector domain given by:

$$\bar{G}(k_s) = \left[\bar{T}_1^{22}(\bar{T}_1^{12})^{-1} + (\overline{g_0}.\,\bar{T}_2^{12} - \bar{T}_2^{22})^{-1} + (\overline{g_0}.\,\bar{T}^{11} - \bar{T}^{21})^{-1}\right]^{-1} \quad (5)$$

To calculate the resonant frequency, the determinant must be equal to zero [13]. Although the full-wave analysis can give results for several resonant modes [13, 14], the results for the fundamental and for higher order modes are presented in this study. Note that the spectral domain approach is valued in the antenna design process, because this approach doesn't make assumptions about the structure's geometry or its electromagnetic behavior, allowing very accurate results to be generated.

In the next section, a basic ANN is described briefly, and our application to the calculation of the resonant frequency of an MSA is then explained. The neural model computes the resonant frequency of the equilateral triangular patch antenna, given that this frequency is an important parameter to be determined accurately [16-18]. In fact, microstrip antennas have narrow bandwidths [19] and can only operate effectively in the vicinity of the resonant frequency. The theory presented in this section has considered that the equilateral triangular patch is printed on an isotropic dielectric substrate material. In the conception of Monolithic Microwave Integrated Circuits (MMIC) and printed antennas, anisotropic substrates have been more and more popular. Bearing in mind that many practical substrate materials used in microstrip antennas exhibit a significant amount of anisotropy (intrinsic anisotropy) that can affect the performance of printed antennas, so accurate characterization and design must account for this effect [20, 21]. The anisotropy can also be artificially caused by the substrate fabricating process (manufacturing process) [22]. A significant focus in research on microstrip antennas printed on anisotropic substrates is particularly given on uniaxial anisotropic substrates due to their various benefits, along with their capability of emulating the electromagnetic features of metamaterials [23]. The uniaxial anisotropic material is distinguished by a perpendicular dielectric constant (ε⊥) and a parallel dielectric constant (ε∥) [22-24]. This means that there are two distinct propagation constants, one for TM waves and

another for TE waves. Note that the proposed method can be easily extended to the case of anisotropic substrates by replacing the matrix representation given in (4) with that shown in (9) [25].

III. ANN MODELING

Several areas of microwave engineering use neural network approaches for optimization. There have been several recent publications on the use of ANN techniques in microstrip architectures. The learning algorithm and the ANN design are the two most crucial components in the creation of an ANN model. There are numerous structural designs and structures for ANNs [8-10]. The main advantage of using ANNs in microwave modeling and design is that, using measured or simulated data from microwave devices, ANNs can be trained to learn relevant microwave relationships, which are, otherwise, computationally expensive or for which efficient analytical formulas are not available. Multilayer Perceptrons (MLPs) have been applied successfully in solving some difficult and diverse problems by training them in a supervised manner with a highly popular algorithm known as the error back-propagation algorithm [9]. An MLP has an input layer, one or more hidden layers, and an output layer. Neurons in the input layer act only as buffers to distribute the x_i input to neurons in the hidden layer. Each neuron in the hidden layer adds its x_i input signals after weighing them with the strengths of the respective w_{ji} connections from the input layer and calculates their y_j output as a function f of the sum:

$$y_j = f(\sum w_{ji}\, x_i) \quad (6)$$

where f may be a hyperbolic tangent, sigmoid, or simple threshold function. The output of the neurons in the output layer is also calculated. The train and test data of the ANN synthesis and analysis were obtained from calculations of a spectral model and a computer program using the above mentioned equations.

The resonant frequency of the antenna is determined in the current work as a function of the material's dielectric constant, air separation, and patch side length. As such, this example is ideal for demonstrating the capabilities and attributes of ANNs.

IV. NUMERICAL RESULTS AND DISCUSSION

Tables I and II show the comparison of the resonant frequency of the triangular patch antenna with the theoretical and experimental results taken from the literature. Additionally, we contrasted our computed values with the simulated outcomes [CST], which are displayed in Table III.

TABLE I. COMPARISON OF THE CALCULATED RESONANT FREQUENCIES WITH THE MEASURED DATA FOR AN EQUILATERAL TRIANGULAR PATCH ON A MONOLAYER SUBSTRATE. a = 10 cm, εr = 2.32, h_2 = 1.59 mm.

Mode	Resonance frequency GHz			Error (%)
	Spectral Domain Approach (SDA)	Our results	Measured results [26]	
TM_{10}	1.18	1.2848	1.280	0.37
TM_{11}	2.22	2.2253	2.242	0.74
TM_{20}	2.52	2.5695	2.550	0.76
TM_{21}	3.38	3.3991	3.400	0.03
TM_{30}	3.87	3.8543	3.824	0.79

TABLE II. RESULT COMPARISON OF THE RESONANT FREQUENCIES WITH THE MEASURED DATA OF EQUILATERAL TRIANGULAR MICROSTRIP PATCHES

a mm	h_2 mm	εr	Resonant frequencies f_{01} GHz		
			Measured [27]	Calculated	Our results
42	0.8265	2.4	2.955	2.981	2.963
22	0.8265	2.4	5.587	5.513	5.551
42	1.63	4.4	2.208	2.190	2.211

TABLE III. COMPARISON OF THE CALCULATED RESONANCE FREQUENCIES WITH THE RESULTS SIMULATED BY CST FOR AN EQUILATERAL TRIANGULAR PATCH ON A SUSPENDED SUBSTRATE OPERATING IN DIFFERENT MODES AND FOR DIFFERENT VALUES OF THE AIR SEPARATION. a = 10 cm , εr = 2.32, h_2 = 1.59 mm

Air separation h_1 mm	Mode	Resonance frequency GHz	
		Our results	CST
0.254	TM_{10}	2.4008	2.385
	TM_{11}	4.1583	4.215
	TM_{20}	4.8016	4.720
	TM_{21}	6.3519	6.395
	TM_{30}	7.2023	7.065
0.635	TM_{10}	2.2655	2.255
	TM_{11}	3.9239	3.985
	TM_{20}	4.5310	4.435
	TM_{21}	5.9939	6.055
	TM_{30}	6.7964	6.620

Tables I and II show clearly that our results, calculated using the neural models proposed in this paper, are better than those calculated in the literature. The very good agreement between the measured values and our calculated resonant frequency values supports the validity of the neural model. An excellent match between our predicted resonant frequencies and the simulated values can also be seen in Table III.

We shall examine the structure of an equilateral triangular antenna with an air gap as our second structure. For various substrate materials, the resonance frequency as a function of the air separation h_1 is displayed in Figure 2.

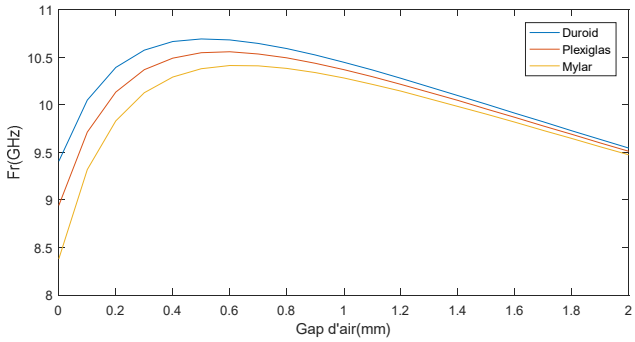

Fig. 2. Resonance frequency of equilateral triangular patch on suspended substrate as a function of air separation. The antenna operates in TM_{10} mode. a = 1.33 cm, h_2 = 0.5 mm, duroid: εr = 2.32, plexiglas: εr = 2.6, mylar : εr = 3.

Resonant frequency is shown to increase quickly with increasing air separation up to a maximum operating frequency for a well-defined air separation (h_{1fmax}). Keep in mind that

with low values of h_1, the impact of the air gap is more noticeable. The resonant frequency will gradually drop as the air gap width increases when the air separation exceeds h_{1fmax}.

Extreme care should be taken when designing an equilateral triangular antenna with a thin air gap, since a small uncertainty in the adjustment of h_1 can result in a significant shift in frequency. Figure 3 shows the resonant frequency of the triangular antenna as a function of the length of the patch side. The initial patch of side a = 6 cm is incremented each time from 1 cm to a final length of 12 cm. In addition to the TM_{10} fundamental mode, we have also indicated in this figure the results of TM_{11} and TM_{20} modes. It is clear from the Figure 3 that increasing the length of the patch side decreases the resonant frequency for the three modes considered.

In Figure 4, we observe that when the permittivity increases the resonance frequency is decreased.

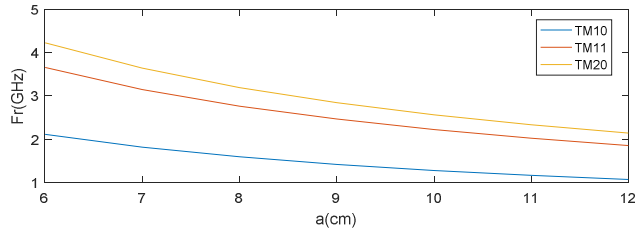

Fig. 3. Resonance frequency of the monolayer equilateral triangular antenna operating in several resonant modes depending on the length of the patch side. εr = 2.32, h = 1.59 mm.

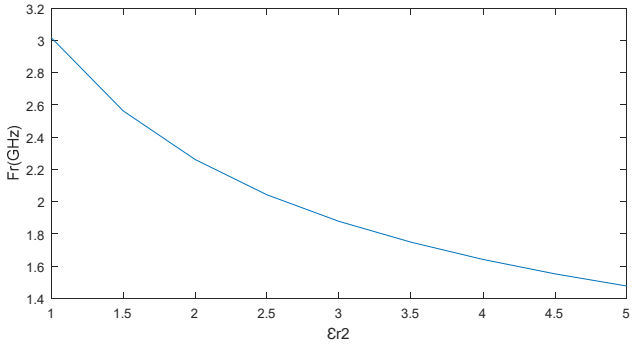

Fig. 4. The effect of the permittivity on the resonance frequency of a triangular monocouch patch. the antenna operates in TM_{10} mode. a = 6 cm, h_2 = 1.59 mm.

V. CONCLUSION

Using an adjustable air gap layer inserted between the ground plane and the substrate, the proposed equilateral triangular patch antenna can achieve tunable resonant frequency characteristic. The proposed antenna was analyzed using the rigorous spectral domain approach. The shortcoming of this approach is the very long calculation time, which makes it incompatible with CAD. In order to solve this problem, we introduced artificial neural networks in conjunction with the spectral method into the analysis of the equilateral triangular patch antenna on suspended and single substrate. Numerical results were obtained for the fundamental and for higher order modes. Our results were compared with and theoretical values available in the literature, and were found to be in very good agreement.

Computations showed that the effect of the air separation on the resonant frequency of the equilateral triangular patch antenna is significant, especially for thin air gap layer. Moreover, particular attention should be taken when designing a thin air gap equilateral triangular patch antenna as a small uncertainty in the air gap setting can cause significant frequency degradation. The strengths of the proposed method are: it is a faster technique compared to the spectral domain approach, it has accuracy similar to that of full-wave methods, it is cost effective, and has the possibility of easily extending to the analysis of equilateral triangular patch printed on anisotropic substrate material.

REREFENCES

[1] M. Shaw, N. Mandal, and M. Gangopadhyay, "A compact circularly polarized isosceles triangular microstrip patch antenna with parasitic elements for multiband application," *Microwave and Optical Technology Letters*, vol. 62, no. 10, pp. 3275–3282, 2020, https://doi.org/10.1002/mop.32445.

[2] R. Chopra and G. Kumar, "High gain broadband stacked triangular microstrip antennas," *Microwave and Optical Technology Letters*, vol. 62, no. 9, pp. 2881–2888, 2020, https://doi.org/10.1002/mop.32372.

[3] A. Mhamdi, S. Bedra, R. Bedra, and S. Benkouda, "CAD cavity model analysis of high Tc superconducting rectangular patch printed on anisotropic substrates," in *5th International Conference on Electrical Engineering - Boumerdes*, Boumerdes, Algeria, Oct. 2017, pp. 1–4, https://doi.org/10.1109/ICEE-B.2017.8192168.

[4] S. Benkouda, M. Amir, T. Fortaki, and A. Benghalia, "Dual-Frequency Behavior of Stacked High TcSuperconducting Microstrip Patches," *Journal of Infrared, Millimeter, and Terahertz Waves*, vol. 32, no. 11, pp. 1350–1366, Nov. 2011, https://doi.org/10.1007/s10762-011-9842-1.

[5] A. Mahamdi, "Modelisation et optimisation des structures rayonnantes par des methodes hybrides," Ph.D. dissertation, Constantine 1 University, Constantine, Algeria, 2021.

[6] A. Mahamdi, S. Benkouda, S. Aris, and T. A. Denidni, "Resonant Frequency and Bandwidth of Superconducting Microstrip Antenna Fed through a Slot Cut into the Ground Plane," *Electronics*, vol. 10, no. 2, Jan. 2021, Art. no. 147, https://doi.org/10.3390/electronics10020147.

[7] A. Mahamdi, S. Benkouda, M. Amir, and S. Bedra, "Study of two-layered circular patch using moment method and genetic algorithms," *International Journal of Electrical and Computer Engineering*, vol. 9, no. 6, pp. 5368–5375, Dec. 2019, https://doi.org/10.11591/ijece.v9i6.pp5368-5375.

[8] R. K. Mishra and A. Patnaik, "Neurospectral computation for complex resonant frequency of microstrip resonators," *IEEE Microwave and Guided Wave Letters*, vol. 9, no. 9, pp. 351–353, Sep. 1999, https://doi.org/10.1109/75.790471.

[9] C. Christodoulou and M. Georgiopoulos, *Applications of Neural Networks in Electromagnetics*. Norwood, MA, USA: Artech House, 2000.

[10] S. K. Jain, A. Patnaik, and S. N. Sinha, "Design of custom-made stacked patch antennas: a machine learning approach," *International Journal of Machine Learning and Cybernetics*, vol. 4, no. 3, pp. 189–194, Jun. 2013, https://doi.org/10.1007/s13042-012-0084-x.

[11] A. Mahamdi, S. Benkouda, and S. Bedra, "Artificial Neural Network Model Analysis of Tunable Circular Microstrip Patch Antenna," in *International Conference on Advanced Systems and Emergent Technologies*, Hammamet, Tunisia, Mar. 2019, pp. 229–233, https://doi.org/10.1109/ASET.2019.8870988.

[12] A. Mahamdi, S. Benkouda, and S. Bedra, "Fast and Accurate Model to Determine the Resonant Characteristics of Elliptical Microstrip Patch Antenna," in *International Conference on Advanced Systems and*

Emergent Technologies, Hammamet, Tunisia, Mar. 2019, pp. 234–237, https://doi.org/10.1109/ASET.2019.8871019.

[13] S. Bedra, R. Bedra, S. Benkouda, and T. Fortaki, "Superstrate loading effects on the resonant characteristics of high Tc superconducting circular patch printed on anisotropic materials," *Physica C: Superconductivity and its Applications*, vol. 543, pp. 1–7, Dec. 2017, https://doi.org/10.1016/j.physc.2017.09.006.

[14] S. Bedra, S. Benkouda, and T. Fortaki, "Analysis of a circular microstrip antenna on isotropic or uniaxially anisotropic substrate using neurospectral approach," *COMPEL: The International Journal for Computation and Mathematics in Electrical and Electronic Engineering*, vol. 33, no. 1/2, pp. 567–580, Jan. 2014, https://doi.org/10.1108/COMPEL-10-2012-0225.

[15] S. Bedra, R. Bedra, S. Benkouda, and T. Fortaki, "Analysis of HTS circular patch antennas including radome effects," *International Journal of Microwave and Wireless Technologies*, vol. 10, no. 7, pp. 843–850, Sep. 2018, https://doi.org/10.1017/S175907871800034X.

[16] S. Bedra, S. Benkouda, M. Amir, and T. Fortaki, "Resonant Frequency of Tunable Microstrip Ring Antenna Printed on Isotropic or Uniaxially Anisotropic Substrate," *Advanced Electromagnetics*, vol. 2, no. 2, pp. 6–9, Aug. 2013, https://doi.org/10.7716/aem.v2i2.194.

[17] M. Hassad, A. S. Boughrara, and T. Fortaki, "Full-wave Analysis of Rectangular Microstrip Antenna Printed on Electric-Magnetic Uniaxial Anisotropic Substrates," *International Journal of Future Generation Communication and Networking*, vol. 7, no. 4, pp. 183–194, Aug. 2014, https://doi.org/10.14257/ijfgcn.2014.7.4.17.

[18] R. Bedra, S. Bedra, and T. Fortaki, "Analysis of elliptical-disk microstrip patch printed on isotropic or anisotropic substrate materials," *International Journal of Microwave and Wireless Technologies*, vol. 8, no. 2, pp. 251–255, Mar. 2016, https://doi.org/10.1017/S1759078714001433.

[19] S. Bedra and T. Fortaki, "Effects of superstrate layer on the resonant characteristics of superconducting rectangular microstrip patch antenna," *Progress In Electromagnetics Research C*, vol. 62, pp. 157–165, 2016, https://doi.org/10.2528/PIERC15122902.

[20] A. S. Boughrara, S. Benkouda, A. Bouraiou, and T. Fortaki, "Study of Stacked High Tc Superconducting Circular Disk Microstrip Antenna in Multilayered Substrate Containing Isotropic and/or Uniaxial Anisotropic Materials," *Advanced Electromagnetics*, vol. 8, no. 3, pp. 1–5, May 2019, https://doi.org/10.7716/aem.v8i3.583.

[21] A. Bediaf *et al.*, "Unlocking Enhanced Bandwidth for 5G Microstrip Antennas: A Comparative Analysis of Substrate Anisotropy and Thickness Manipulation Techniques," in *International Conference on Electrical Engineering and Advanced Technology*, Batna, Algeria, Nov. 2023, vol. 1, pp. 1–4, https://doi.org/10.1109/ICEEAT60471.2023.10426321.

[22] S. Bedra, R. Bedra, S. Benkouda, and T. Fortaki, "Study of an Inverted Rectangular Patch Printed on Anisotropic Substrates," *IETE Journal of Research*, vol. 68, no. 2, pp. 1056–1063, Mar. 2022, https://doi.org/10.1080/03772063.2019.1634497.

[23] M. Bedra, S. Bedra, T. Fortaki, D. Arar, D. Benatia, and A. Bediaf, "Theoretical investigation of HTS compact microstrip antennas printed on anisotropic substrates using hybrid cavity model," *Cryogenics*, vol. 143, Oct. 2024, Art. no. 103935, https://doi.org/10.1016/j.cryogenics.2024.103935.

[24] T. Fortaki, L. Djouane, F. Chebara, and A. Benghalia, "On the Dual-Frequency Behavior of Stacked Microstrip Patches," *IEEE Antennas and Wireless Propagation Letters*, vol. 7, pp. 310–313, 2008, https://doi.org/10.1109/LAWP.2008.921344.

[25] T. Fortaki and A. Benghalia, "Rigorous full-wave analysis of rectangular microstrip patches over ground planes with rectangular apertures in multilayered substrates that contain isotropic and uniaxial anisotropic materials," *Microwave and Optical Technology Letters*, vol. 41, no. 6, pp. 496–500, 2004, https://doi.org/10.1002/mop.20183.

[26] J. Dahele and K. Lee, "On the resonant frequencies of the triangular patch antenna," *IEEE Transactions on Antennas and Propagation*, vol. 35, no. 1, pp. 100–101, Jan. 1987, https://doi.org/10.1109/TAP.1987.1143960.

[27] A. Gadda, S. Bedra, C. Agaba, S. Benkouda, R. Bedra, and T. Fortaki, "Computer-Aided Design of Superconducting Equilateral Triangular Patch on Anisotropic Substrates," *Progress In Electromagnetics Research M*, vol. 86, pp. 203–212, Nov. 2019.